Environ Geochem Health
https://doi.org/10.1007/s10653-022-01407-5

ORIGINAL PAPER

# Geochemical and mineralogical characterization of Ria de Aveiro (Portugal) saltpan sediments for pelotherapy application

**Lara Almeida · Fernando Rocha · Carla Candeias**

Received: 26 May 2022 / Accepted: 20 September 2022


**Abstract** The present study aims to characterize sediments textural, geochemical and mineralogical composition used in a SPA for pelotherapy applications. Six samples were collected in two areas of an open-air saline SPA, a former saltpan in Ria de Aveiro (Portugal). Sampling areas are predominantly composed by recent alluvium that had been affected by chemical industrial effluents for over 50 years. Samples < 2000, 63, and 2 µm fractions were analyzed by X-ray Diffraction (XRD) and X-ray Fluorescence (XRF), for identification of mineral phases and chemical composition. SEM analysis was used for individual particles morphological characterization and chemical semi-quantification. Texture, mineral phases and chemical composition showed the influence of SPA pond beneficiation works. The two SPA areas revealed distinct mineral phases, one with higher quartz content, and the other with higher halite content, consistent with their environmental conditions. Illite constituted the most abundant mineral phase of the clay fraction. Preliminary results suggested concentrations of potential toxic elements (e.g., As, Cd) above reference values, representing a risk to the ecosystem and humans.

L. Almeida · F. Rocha · C. Candeias (✉)
GeoBioTec Research Unit, Geosciences Department, University of Aveiro., Campus de Santiago, 3810-193 Aveiro, Portugal
e-mail: candeias@ua.pt

**Keywords** Geochemistry · Mineralogy · PTEs · Pelotherapy · Ria de Aveiro

## Introduction

Pelotherapy is the topical application of peloids for therapeutic or cosmetic purposes (Veniale et al., 2004), where peloids are usually applied in the form of poultices on a certain area of the body (e.g., back, arms, legs), at a temperature 40–45 °C, that enhance therapeutical benefits. Treatments commonly consist of peloids application on a body area, after covered with impermeable fabric and blanket to prevent water evaporation and to allow heat dissipation. The duration of peloids application usually varies between 20 to 30 min (Carretero, 2020a; Gomes, 2018).

Gomes et al. (2013) proposed a definition for peloids as "a maturated mud or muddy dispersion with healing and/or cosmetic properties, composed of a complex mixture of fine-grained natural materials of geologic and/or biologic origins, mineral water or sea water, and commonly organic compounds from biological metabolic activity". These materials were classified according to its origin by: (a) purely mineral; (b) alluvial and marine, characterized by organic matter (e.g., algae, diatoms, bacteria); (c) intermediate group of terrestrial peloids; (d) mainly vascular-vegetable origin, e.g., moors; (e) marine origin; and (f) derived from petroleum deposits. In short, peloids are a mixture of solid

Published online: 04 October 2022

inorganic/organic materials and a liquid that can contains a gaseous phase, such as $CO_2$ or radon (Gomes et al., 2013).

Peloids have been used for therapeutical or cosmetic purposes since ancient times, and their potential beneficial effects on human health, have been studied extensively, especially for rheumatological and dermatological applications (e.g., Argenziano et al., 2004; Bastos et al., 2020; Codish et al., 2005; Karakaya et al., 2010; Quintela et al., 2012; Viseras et al., 2019). Peloids can have natural origin and maturation processes, or human intervention on both the mixture and maturation. These pastes are continuously in transformation during maturation, a process that includes the solid–liquid mixture and organic changes that are dependent of their physical, biological, mineral, and chemical properties (Gomes et al., 2013). During this process, biological growth (e.g., diatoms, bacteria, protozoa) can occur varying with mixture characteristics, and phyllosilicate content (Carretero, 2020b). For example, diatoms present in the matured paste can produce proteins and lipids that enhance anti-inflammatory properties (Tolomio et al., 1999).

Characterization of peloids by different techniques of sediments and waters initial form is essential for the definition of potential peloids mixture (Carretero, 2020a). Solid materials consist of fine-grained minerals that may contain varying amounts of other mineral phases (e.g., quartz, feldspar, mica, calcite) and organic matter (Baschini et al., 2010; Vieira et al., 2008). Previous peloids studies, both in solid and water components, reported the presence of potentially toxic elements (PTEs) what can represent a risk to human health once they can be released during applications and to the skin and blood systems (Kikouama et al., 2009; Pozo et al., 2010; Williams et al., 2008).

In Portugal, pelotherapy has a long tradition both in rivers, lakes, and saline environments, such as Porto de Mós beach and Ria de Aveiro lagoon. In the present study, highly saline sediments that suffered natural maturation processes were studied. Study area is a former saltpan recently adapted to a SPA were these peloids have been used empirically with no medical supervision. Sediments are hand collected and applied on the skin, by its users. The aims of this study were to: (a) characterize chemical, mineralogical, and textural composition of the sediments; and (b) quantify potentially toxic elements (PTEs) present and estimate their dermal risk.

## Materials and methods

### Study area

Marinha da Noeirinha SPA, is located on a former saltpan at Ria de Aveiro (Portugal), that was recently adapted to an artificial peri-urban SPA with two distinct areas (Fig. 1). Area 1 is a shallow limited artificial beach with marine waters with tidal influence, that has occasional inputs of allochthonous sand on its margins that aim the SPA artificial beach conditions beneficiation. Area 2 is located on a recovered artificial saltpan, having salt production from March to October. This SPA area is used for direct application of salt in shallow ponds, with 10–20 cm saltwater depth. Both areas are used during summer periods both for bathing and empirical sediments applications, without medical supervision.

Ria de Aveiro is a shallow coastal lagoon, with a mixture of marine and fresh waters, located on the NW Portuguese coast, separated from the sea by a sand bar (Dias et al., 1999). The lagoon is connected to the Atlantic Ocean by a narrow artificial channel with the influence of Vouga river flow, that supplies Ria de Aveiro with fresh water and sediments (Dias et al., 2000; Mil-Homens et al., 2014). Ria de Aveiro lagoon has a residual circulation, being considered mainly tidal dominated (Dias et al., 2003).

Geologically, the area is located in the Aveiro Sedimentary Basin, deployed in the Lusitanian Basin. Local formations are stratigraphically dated from the Quaternary, represented by modern deposits: alluviums, beach and dune sands, arranged in layers of various thicknesses. Specifically, alluviums predominate, composed by silt, sandy and micaceous silt, silt with shells, muddy and coarse sands that are settle on the existing substrate (Teixeira & Zbyszewski, 1976).

Ria de Aveiro suffered water quality degradation due to chemical anthropogenic inputs (Lopes et al., 2005). Estarreja Chemical Complex (ECC), located 10 km N of Aveiro urban area, is the second largest chemical area in Portugal, and the Portuguese Environmental Agency highlighted the need for rehabilitation priority actions. For decades occurred unmonitored industrial direct discharges


**Fig. 1** Study area location and surrounding environmental context (adapt. Google® maps, 2022)

to the lagoon, without environmental concerns, that contaminated not only the nearby areas but also further away by tidal transport of potentially toxic elements (PTEs). Gadelha et al. (2019) suggested that the lack of human activities control is reflected in the lagoon waters and sediments quality, with high PTEs concentration, e.g., As, Pb and Zn, found also in distant areas from ECC source area (Costa & Rydin, 2001).

Near Marinha da Noeirinha SPA area there are diverse infrastructures, such as, to the East, a freight train line, and a highway, and to the West a former harbor and fish auction, that disturbed the environmental conditions and contribute to contamination (Fig. 1). According to Martins et al. (2013) and Pastorinho et al. (2012), Ria de Aveiro sediments act as a sink for many potentially toxic elements (PTEs) and organic matter. Martins et al. (2013), analyzed the distribution of PTEs in Ria de Aveiro sediments and concluded that Aveiro urban Canals is where the highest concentration of Zn, Pb and Cu were found, an enrichment linked to the past chemical industrial discharges but also to maritime transport of supplies to and from the city.

## Sampling, samples preparation and analysis

A total of six sediment samples were collected in the SPA areas 1 and 2 (Fig. 1), in different periods of 2020 and 2021 (Table 1). Samples A1a and A1b were collected before beach improvement works of Area 1, with the input of allochthonous sand on its margins. Samples A1c and A1d were collected after this intervention. Sample groups A1a, A2a and A1d, A2d were collected simultaneously, in the first and last sampling campaigns, respectively. Area 2 was not submitted to any beneficiation works.

After collection, samples were stored in individual referenced polyethylene bags until laboratorial

**Table 1** Samples description

| ID | Area | Period |
|---|---|---|
| A1a | 1 | Spring 2020 |
| A1b | 1 | Winter 2021 |
| A1c | 1 | Summer 2021 |
| A1d | 1 | Autumn 2021 |
| A2a | 2 | Spring 2020 |
| A2d | 2 | Autumn 2021 |

preparation and analyses. In the laboratory, total samples were wet sieved to obtain < 63 μm fraction (silt) and by sedimentation, using Stokes' Law, to obtain < 2 μm fraction (clay). Sediments were oven dried (~ 40 ºC), homogenized, and a portion grounded on an agate mill for chemical and mineralogical analysis. Size distribution of the silt fraction was obtained using an X-ray grain size analyzer, Micromeritics® Sedigraph III Plus (University of Aveiro—UAVR). This textural characterization method is based on the absorption of X-radiation (Beer-Lambert law) and the sedimentation theory (Stokes' law).

Sediments physical parameters were determined: color, using Munsell color chart (Munsell, 2009); pH with method, using a calibrated pH meter Hanna HI 9126 model, whereby the suspension of samples was made up in five times its volume of a 0.01 mol/l solution of calcium chloride ($CaCl_2$); electrical conductivity (EC) was determined by the same method of pH, using a calibrated conductivity meter Hanna HI 9033 model; and organic matter (OM) using procedure proposed by Reeuwijk (2002), consisting of burning organic material and the relation of weights before and after burning process.

Samples geochemical composition was achieved by X-ray fluorescence (XRF) carried with a Panalytical Axios spectrometer PW4400/40 X-ray (Marvel Panalytical, Almelo, The Netherlands) operating on an Rh tube under argon/methane (UAVR). Limits of detection (LOD) were As 4.1; Cd 3.9; Co 4.5; Cr, Ni 2.0; Cu, 2.8; Pb 1.7; Zn 1.3, and Zr 0.8 mg/kg.

Mineral phases were determined using a Phillips/Panalytical power diffractometer, model X'Pert-Pro MPD, carrying an automatic slit (UAVR). XRD makes use of Cu-X-ray tube operated at 50 kV and 30 mA, which allowed data to be collected from 2 to 70° 2$\theta$ with a step size of 1° and a counting interval of 0.02 s. XRD analysis (qualitative and semi-quantitative) was carried out on total sample, and silt (< 63 μm) and clay (< 2 μm) fractions, according to Brindley and Brown (1980), Galhano et al. (1999) and Oliveira et al. (2002).

Individual particles morphology and size determination was performed with an Hitachi S-4100 scanning electron microscope (SEM), model VEGA LMU, operating in high and low vacuum and capable of image acquisition through secondary and back-diffused electron detectors (UAVR). Particles semi-quantitative chemical characterization was determined by elemental chemical analysis using an Energy Dispersive Spectrometer (EDS). Mix of protocols allowed the individual identification of inorganic insoluble particles (Wu et al., 2016).

Internal standards, certified reference material and quality control blanks were used for monitoring the precision and accuracy of the analyses and digestion procedures. Samples revealed results were within the 95% confidence limits and the Relative Standard Deviation was between 5 and 10%.

## Data analysis

Sediment Quality Guidelines (SQG) have been used to evaluate contamination degree in sediments (Zhang et al., 2016). The threshold (TEL) and the probable effect (PEL) levels are broadly used to assess sediment toxicity (Zhao et al., 2016). Between the TEL and PEL, is the possible effect range within which adverse effects occasionally occur. In this study, values used were, TEL, or concentration of a pollutant below which adverse effects are not expected to occur, were As = 5.9, Cd = 0.596, Cr = 37.4, Cu = 35.7, Ni = 18, Pb = 35, and Zn = 123 (Smith et al., 1996); and PEL, or a pollutant concentration limit above which adverse effects are expected to occur more often than not, were As = 17, Cd = 3.53, Cr = 90, Cu = 197, Ni = 36, Pb = 91.3, and Zn = 315 (Smith et al., 1996).

Toxic Risk Index (TRI) is a method to evaluate a system ecotoxicity taking in consideration TEL and PEL levels. The potential sediment acute toxicity is calculated by $\mathrm{TRI} = \sum_{i=1}^{n} \mathrm{TRI}_i$, where $\mathrm{TRI}_i = \sqrt{[(C_i/\mathrm{TEL}_i)^2 + (C_i/\mathrm{PEL}_i)^2]/2}$, with $C_i$ the $i$ pollutant concentration and $n$ the number of selected pollutants (Long et al., 2006). Toxic risk degree is classified as, no toxic risk (TRI ≤ 5), low toxic risk (5 < TRI ≤ 10), moderate toxic risk (10 < TRI ≤ 15), considerable toxic risk (15 < TRI ≤ 20), and very high toxic risk (TRI > 20) (Zhang et al., 2016).

Contamination factor (CF) and contamination degree (CD) are parameters used to assess the sediments contamination. Contamination Factor (CF) express the level of metal contamination in sediment and is calculated as $\mathrm{CF} = \mathrm{Cm}_{\mathrm{sample}}/\mathrm{Cm}_{\mathrm{background}}$, where $\mathrm{Cm}_{\mathrm{sample}}$ represents the amount of a given metal in the sediments samples and $Cm_{background}$ is the value of the metal that is equivalent to the

upper continental crust (UCC) in the studied sediments (Avumadi et al., 2019; Rasul and Al-jaleel, 2022). CF is classified as $0 \leq CF < 1$ low, $1 \leq CF < 3$ moderate, $3 \leq CF < 6$ high, and $6 \leq C$ very high Contamination Factor (Håkanson, 1980; Loska et al., 1997). Contamination degree (CD) is defined as the sum of the CF for the eight metal species (Håkanson, 1980) and it is calculated using the following formula $C_D = C_D = CD = \sum_{i=1}^{n=7} CF_i$. CD is classified as $0 \leq CD < 6$ low, $6 \leq CD < 12$ moderate, and $12 \leq CD < 24$ considerable, and $24 \leq CD$ very high Contamination Degree (Håkanson, 1980).

Risk assessment was calculated taking into consideration that SPA visitors, both children and adults, are exposed to sediments through three main routes: ingestion, inhalation, and dermal absorption. Nevertheless, only dermal adsorption for the present study was considered. Non-carcinogenic hazard (systemic toxicity) and carcinogenic risk for potentially toxic element (PTE) considered were calculated considering formulas and reference toxicity levels, as extensively described in RAIS (2022). Adjustable parameters used: ingestion rate for adults 200 and children 100 mg/d; inhalation rate of 7.6 and 20 m3/d for children and adults, respectively; exposure frequency of 30 d/yr; exposure period (EP) of 3 and 10 years for non-carcinogenic effects in children and adults, respectively; lifetime (LT) of 70 years; average body weight of 15 (children) and 60 kg (adults); average time for non-carcinogenic effects = EP × 365 days; exposed skin area of 2800 and 5700 $cm^2$ for children and adults, respectively; skin adherence factor of 0.2 and 0.07 $mg/cm^2$ for children and adults, respectively, dermal absorption factor of 0.001 for all selected PTE (As, Cd, Co, Cr, Cu, Pb, Mn, Ni, Pb, Zn and Zr), particulate emission factor of $1.36 \times 109$ $m^3/kg$; soil dermal contact factor-age-adjusted of 362 mg.yr/kg.d, average of carcinogenic effects time = LT × 365 days; and exposure time of 8 h/d (RAIS, 2022). Non-carcinogenic hazard was estimated by the Hazard Quotient (HQ) for systemic toxicity for each PTE and exposure route. The cumulative non-carcinogenic Hazard Index (HI) is the sum of HQ routes and/or variables, was not considered. If HI > 1 non-carcinogenic effects might occur once exposure concentration exceeds the reference dose. Dermal carcinogenic risk, or the probability of an individual to develop any type of cancer over a lifetime in result of dermal exposure to PTE, was evaluated by the sum of total carcinogenic risk of the considered elements. Carcinogenic target risk is 1.00E − 06, and risk if > 1.00E − 04 is considered unacceptable (RAIS, 2022).

Statistical analysis was performed by using descriptive statistics, *t*-student test, and cluster analysis were performed by using SPSS v.27® software (IBM, USA). Cluster analysis was applied with Ward's method and Euclidean distance as a measure of similarity.

## Results and discussion

Samples textural classification is presented in Fig. 2. Area 1 sediments, before improvement works, were classified chronologically as clay loam (spring) and loam (winter), while after the beneficiation activities were classified as sand (summer) and loamy sand (autumn). Results reflected the impact of climatic conditions in all samples texture but also, SPA improvement works on short term (A1c) and some months later (A1d), with tidal and climatic influence on materials transport. Sample A1c presented a sand fraction of 90.0% while sample A1d presented a small sand sized reduction (83.2%). These samples presented a mud fraction (silt + clay) of 10.0 and 16.8%, respectively, much lower that sand content, suggesting poor reactivity (specific surface). Samples A1a and A1b were the ones with lowest sand fraction content, 27.7 and 23.6%, respectively. Sample A1a

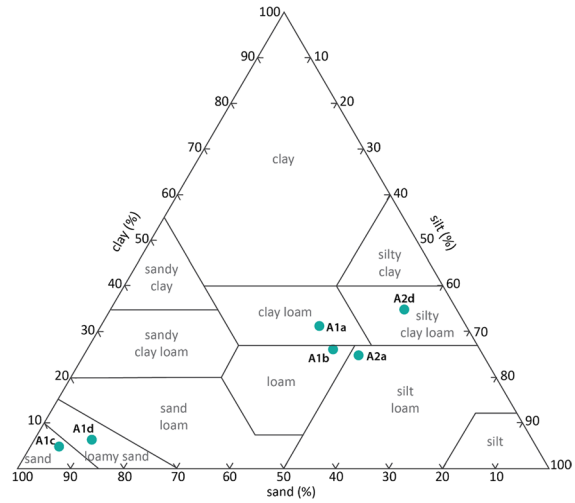


**Fig. 2** Samples textural classification

mud fraction was 72.3%, while sample A1b mud fraction was 76.4%, indicative of suitable reactivity, what allow handling and pleasant feeling when applied on the skin. There is a need of time, with tidal and climate influence, for sediments to recover their initial texture after beneficiation works on this SPA area. Sediments from Area 2 were classified as silty clay loam and silt loam, being mud fraction the most significant, with 72.3 and 90.1%, in samples A2a and A2d, respectively, revealing applicable specific surface for handling.

Samples mineral phases identified are presented in Fig. 3 and include phyllosilicates (e.g., micas/illite, chlorite, kaolinite, smectite), quartz ($SiO_2$), feldspars (plagioclase ($(Na,Ca)[(Si,Al)AlSi_2]O_8$), K feldspar ($KAlSi_3O_8$)), carbonates (calcite ($CaCO_3$)), anhydrite ($CaSO_4$), jarosite ($KFe^{3+}{}_3(SO_4)_2(OH)_6$)), zeolites, opal *C*/CT ($SiO_2{\cdot}nH_2O$), halite (NaCl), and iron oxides such as magnetite-maghemite ($Fe_3O_4$-$\gamma$-$Fe_2O_3$). Quartz was the dominant mineral phase in all samples, while zeolites were only identified in sample A1a. Area 1 total sample minerals were ordered quartz > Σ phyllosilicates > feldspars > carbonates > magnetite-maghemite > > halite > opal *C*/CT > zeolite, while in silt fraction quartz > feldspars > Σ phyllosilicates > carbonates > halite > opal *C*/CT > magnetite-maghemite. Sample A1c presented significant differences from others ($p < 0.05$), with the highest quartz content in total fraction 84.8%) and minor amounts of other minerals, in accordance with the textural classification (Garzanti, 2019). The high content of clay, one of the primary products of chemical weathering, reflected the environmental conditions of these samples. Results were in line with other studies in Ria de Aveiro (e.g., Abrantes et al., 2005; Martins et al., 2014). Area 2 total sample mineral phases were ordered quartz > Σ phyllosilicates > halite > feldspars > carbonates > magnetite-maghemite > opal *C*/CT, while in silt fraction quartz > Σ phyllosilicates > feldspars > halite > carbonates > magnetite-maghemite > opal *C*/CT. These area samples halite higher content reflected the artificial saltpan clayey bottom influence and human activities to promote salt production.

Clay fraction identified mineral phases revealed the presence of illite ($(K_{0.65}Al_2[Al_{0.65}Si_{3.35}O_{10}](OH)_2$) > kaolinite ($Al_2(Si_2O_5)(OH)_4$) > > smectite ($((Na,Ca)_{0.33}(Al,Mg)_2(Si_4O_{10})(OH)_2{\cdot}nH_2O$) > chlorite ($(Mg, Fe)_3(Si, Al)_4O_{10}(OH)_2{\cdot}(Mg, Fe)_3(OH)_6$) (Table 2). Illite high content reflected the temperate climate of the source area, and showed slightly higher crystallinity, with a discrete lateral heterogeneity while the others clay minerals showed low/medium crystallinity with no significant variation, in general (Oliveira et al., 2002; Rocha et al., 2005). Illite, usually a major constituent of ancient mud rocks, is formed from weathering of K and Al-rich materials (e.g., muscovite, feldspars) in high pH conditions.

**Table 2** Clay fraction mineralogical phases identified

| | kaolinite | illite | smectite | chlorite |
|---|---|---|---|---|
| A1a | + | ++ | tr | |
| A1b | | +++ | | |
| A1c | + | +++ | | |
| A1d | ++ | +++ | | |
| A2a | ++ | +++ | tr | |
| A2d | + | +++ | | tr |

*tr* trace

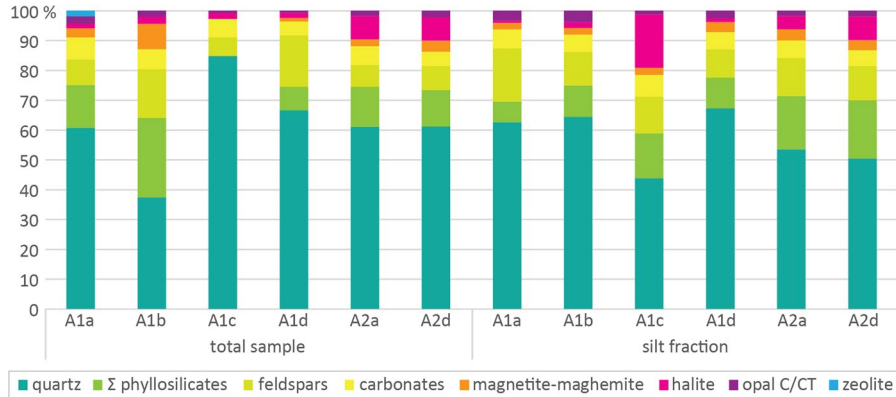


**Fig. 3** Mineralogical composition of total sample and silt fraction

Illite K, Ca, or Mg interlayer cations avoid $H_2O$ into the structure, suggesting that these clays are non-expanding. According to Carretero (2020a) mud samples with high quartz, carbonates, such as calcite, and illite content have high therapeutical applicability. The presence of quartz and carbonates can usefully contribute to application on physiotherapy and cosmetic technologies (Glavaš et al., 2017; Nissenbaum et al., 2002).

Total samples physical parameters are presented in Table 3. pH ranged 5.9 to 7.97. These results are in line with those of Moreira et al. (1993), with pH ranging 6.8 to 8.9 (closely related to $O_2$), and Martins et al. (2014) ranging 4.2 to 9.9. Martins et al. (2014) associated the lowest pH values to inland lagoon areas near freshwater sources. Lower electrical conductivity (EC) was found in sample A1c, ranging 4.0, while higher values were found in more saline waters (11.7 and 22.4 mS/cm). Electrical conductivity is also closely related to particles grain size. Clay particles result in increased surface area per volume unit or per mass unit, where significant cations can be adsorbed, which highlight that clay particles have significant EC (Uddin, 2008). The present study results were in line with studies carried out in Turkey, with high EC peloids (Özay et al., 2020).

Sediment samples color varied from light yellowish brown to dark grayish brown, what can be attributed to the variable OM content (0.60 to 4.88%). OM content reflected the environmental context where sediments may act as sink. According to Vodyanitskii and Savichez (2017) OM is the basic and most important pigment to give dark color and is the most common cause of changes that occur in color indicator. Burdige (2007) considered that marine OM generally consist of debris of phytoplankton or detritus, whose chemical composition is predominantly proteins, carbohydrates and lipids. Living biomass, plant litter is part of terrestrial organic matter, the latter consisting largely of highly altered and degraded remains of terrestrial biomass. Beside humic acids, the presence of microorganisms in peloids may also explain the high OM content (Tserenpil et al., 2010). Lowest OM content, and lightest color, were found in sample A1c, sample classified as sand due to anthropogenic sand input, in agreement with the study done by Hossain et al. (2014).

Individual particles morphology and identification are presented in Figs. 4 and 5. Is common the presence of microorganisms in saline environments and a recent study in Spain also suggested it (Fernández-Moreno et al., 2022). Considering Potopova and Charles (2003) who classified EC as an important contributor to diatoms (biogenic silica) distribution and given EC values measured in these samples, the presence of microorganisms founded in all samples in a significant number was expected. Resende et al. (2005) studied the ecological preference of diatoms in Ria de Aveiro and concluded that their distribution along the lagoon was mainly controlled by the effect of river inflow and tidal incursion, reflecting the occurrence of diatom species within a relatively wide salinity range. Microorganism abundance can be responsible for sediments color and OM content. Particles enriched in Fe, Cu, Ti and Pb, were also identified, in agreement with previous studies that suggested sediments metal contamination (Martins et al., 2010, 2013). The presence of NaCl particles and particles covered with salts reflected the saline conditions of sampling areas.

Samples major elements concentration and lost on ignition (LOI) is presented in Table 4. There are statistically significant differences between fractions on $Al_2O_3$, MgO, $SO_3$ and $TiO_2$ mean concentrations ($p < 0.05$), with higher content in silt fraction. The highest $Na_2O$ and Cl concentration was found in both fractions A2a and A2d collected on the saline pond, and in sample A1b collected during wintertime in low

**Table 3** Physical parameters of total samples

| Var | A1a | A1b | A1c | A1d | A2a | A2d |
|---|---|---|---|---|---|---|
| pH | 7.45 | 5.9 | 7.97 | 6.47 | 7.3 | 7.32 |
| EC | 7.9 | 7.8 | 4.0 | 6.7 | 22.4 | 11.7 |
| OM | 4.35 | 4.73 | 0.60 | 2.22 | 4.88 | 1.41 |
| Color* | Grayish brown | Dark grayish brown | Light yellowish brown | Grayish brown | Grayish brown | Gray |

*EC* electrical conductivity (ms/cm); *OM* organic matter (%)

*Munsel (2009).

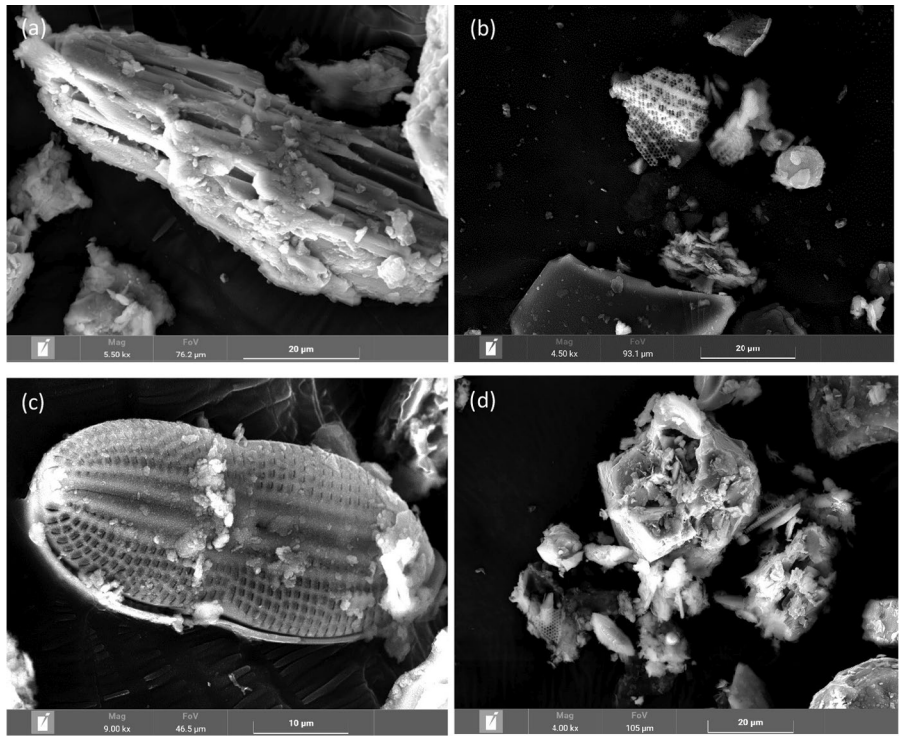


**Fig. 4** SEM images of Area 1 samples A1a to A1d: **a** particle enriched in Fe, covered with diverse smaller particles, including NaCl and $SiO_2$; **b** diverse organic (e.g., diatom frustules) and inorganic (e.g., quartz, halite) particles; **c** resuspended benthic specie *Diploneis wiesflogii* covered with $SiO_2$ and NaCl particles; and **d** inorganic and organic mix of particles enriched in $SiO_2$, Cu, Ti, Pb

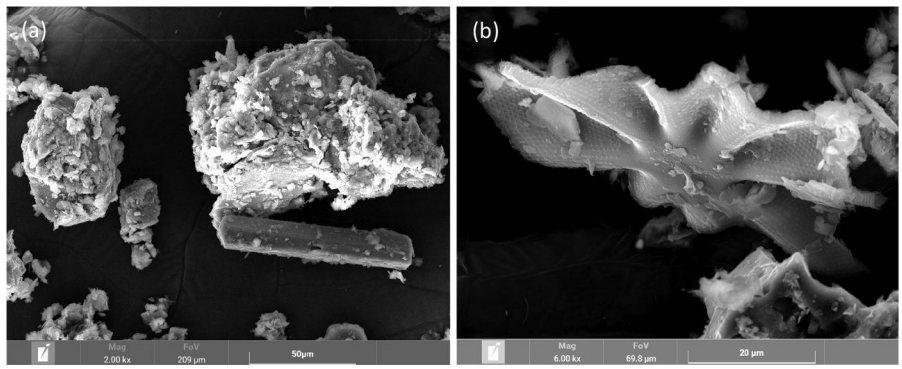


**Fig. 5** SEM images of Area 2 samples A2a and A2d: **a** quartz particles covered with smaller Fe, Mg and Ti enriched particles and also NaCl; and **b** microorganisms covered with salt particles and others enriched in Fe and Mg

tide ($p < 0.01$). These results were related to the presence of halite (NaCl), confirmed by XRD and SEM analysis. Total samples with highest concentrations of $Al_2O_3$ and $K_2O$ are in opposition to lower $Na_2O$ and Cl contents ($p < 0.05$), in agreement with higher presence of phyllosilicates and K feldspars. Additionally, $SiO_2$ presented higher content in Area 1 samples, confirmed by quartz content.

Cluster analysis of total sample (Fig. 6a, b) distinguished 2 clusters (1—samples A1b, A2a and A2d, and 2—samples A1a, A1c and A1d) and 2 major elements groups ($a_1$, $a_2$ and b). Group b corresponded to quartz ($SiO_2$) abundance in all samples. Subgroup $a_2$ is related to halite (NaCl) presence, mostly found in samples from group i. Subgroup $a_1$ incorporated all other major elements related to mineralogical composition of the total samples. Cluster analysis of silt fraction (Fig. 6c, d) formed 2 sample clusters (1—samples A1a, A1b and A1d, and 2—samples A1c, A2a and A2d) and 2 major elements groups ($a_1$, $a_2$ and b). Groups b and $a_2$ suggested the predominance of $SiO_2$ with also significant amounts of NaCl, respectively. Group $a_1$ represented other major

**Table 4** Major elements concentration of total sample and silt fraction (LOI – loss on ignition). In wt.%

| | $Al_2O_3$ | CaO | Cl | $Fe_2O_3$ | $K_2O$ | MgO | MnO | $Na_2O$ | $P_2O_5$ | $SiO_2$ | $SO_3$ | $TiO_2$ | LOI |
|---|---|---|---|---|---|---|---|---|---|---|---|---|---|
| *Total sample* | | | | | | | | | | | | | |
| A1a | 14.94 | 1.19 | 3.58 | 3.70 | 3.49 | 1.82 | 0.02 | 5.68 | 0.13 | 56.45 | 0.94 | 0.61 | 7.22 |
| A1b | 2.77 | 0.17 | 33.62 | 2.88 | 1.08 | 0.34 | 0.02 | 40.94 | 0.02 | 8.54 | 0.42 | 0.29 | 8.75 |
| A1c | 6.26 | 1.90 | 0.78 | 0.52 | 3.03 | 0.47 | 0.01 | 1.48 | 0.07 | 83.20 | 0.29 | 0.10 | 1.84 |
| A1d | 12.55 | 0.49 | 1.62 | 2.79 | 3.05 | 1.42 | 0.02 | 2.68 | 0.11 | 67.39 | 1.25 | 0.47 | 6.06 |
| A2a | 0.65 | 0.23 | 36.62 | 1.56 | 0.25 | 0.12 | 0.01 | 42.45 | 0.01 | 2.20 | 0.23 | 0.11 | 15.45 |
| A2c | 1.39 | 0.20 | 36.83 | 2.43 | 0.70 | 0.25 | 0.01 | 43.07 | 0.01 | 5.25 | 0.33 | 0.20 | 9.44 |
| *Silt fraction* | | | | | | | | | | | | | |
| A1a | 15.77 | 0.93 | 1.27 | 4.06 | 3.67 | 1.83 | 0.02 | 2.27 | 0.14 | 61.99 | 0.75 | 0.72 | 6.41 |
| A1b | 15.16 | 0.42 | 0.85 | 3.69 | 3.52 | 1.58 | 0.02 | 1.87 | 0.12 | 64.34 | 1.42 | 0.71 | 6.08 |
| A1c | 10.79 | 1.09 | 9.73 | 2.69 | 2.67 | 2.80 | 0.02 | 10.29 | 0.11 | 39.28 | 2.13 | 0.43 | 17.84 |
| A1d | 13.38 | 0.41 | 6.26 | 3.42 | 3.23 | 1.55 | 0.02 | 8.71 | 0.10 | 54.64 | 1.41 | 0.63 | 6.11 |
| A2a | 10.21 | 0.36 | 13.75 | 3.21 | 2.52 | 1.55 | 0.02 | 19.92 | 0.06 | 32.92 | 1.05 | 0.47 | 13.71 |
| A2c | 12.89 | 0.32 | 9.32 | 3.43 | 3.13 | 3.25 | 0.02 | 11.78 | 0.08 | 41.94 | 3.51 | 0.54 | 9.48 |

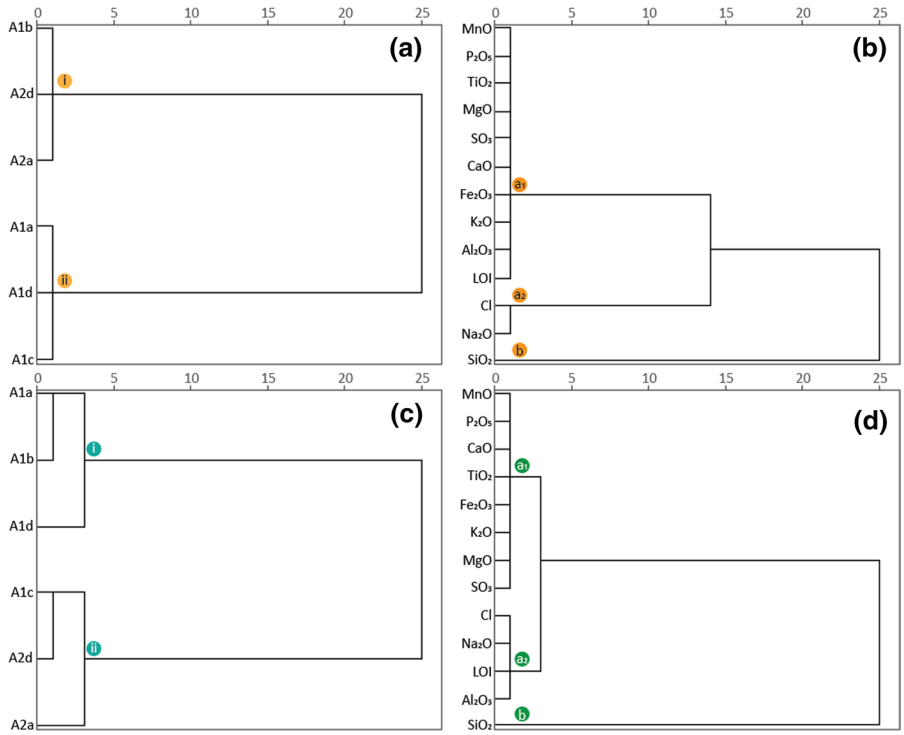


**Fig. 6** Cluster analysis of **a**, **b** total sample, and **c**, **d** silt fraction

elements with significant abundance of aluminous phases and a link to the mineralogical composition of the silt fraction.

According to Ravaglioli et al. (1989), high $Na_2O$/CaO ratio is indicative of swelling 2:1 clay minerals, while a low $Na_2O$/CaO ratio ($Na_2O$/CaO < 1) is typical for non-swelling 2:1 clay minerals. Mineralogy is a property responsible for affecting the swelling properties of clay minerals, that decreases in the presence of CaO enriched minerals (Karakaya et al., 2011). Studied sediments $Na_2O$/CaO ratio showed that only total sample A1c presented a ratio < 1, what can be related to low carbonates content. In these samples, CaO content is related to calcite content, not smectite.

Loss on ignition (LOI) is a common method based to estimate carbonate and organic content in sediments (Heiri et al., 2001; Santisteban et al., 2004). Total sample LOI values ranged 1.84 to 15.45%, corresponding to samples A1c and A2a, respectively, in agreement with highest OM and carbonate content of sample A2a. Silt fraction LOI values ranged 6.08 to 17.84%, corresponding to samples A1b and A1c, respectively, confirming that sample A1c had highest OM and carbonate content.

Materials to be used in pharmaceutical and/or cosmetic products have PTEs concentrations regulated (Infarmed, 2008), avoiding side-effects. Risk assessment of dermal absorption in dermal products is complex. PTEs can occur naturally in sediments and be absorbed during pelotherapy applications (Mascolo et al., 1999). European directives consider that As, Cd, Hg, Pb, Se, Te, and Tl, known for their potential toxicity in humans and environment, must be absent in cosmetic products, including peloids. However, other countries defined a target value for As and Cd (3 mg/kg), and Pb (10 mg/kg), regarded as has impurities (Health Canada, 2012). Health Canada (2012) considered that, (a) inorganic As is the one that represent a carcinogenic risk, but dermal uptake is low, once it doesn't act as a sensitizer; (b) dermal Cd absorption is low (0.5%), and that bigger risk occurs with concentrated solutions in contact with the skin for long periods, due to its bind to epidermal keratin; and (c) inorganic Pb presents a low permeability in the skin, and that children are most susceptible to slit adverse health effect. Other PTEs are considered has impurities in dermal products such as cosmetics, but despite having lower toxicity and associated risk than As, Cd and Pb, must be also limited (European regulation 85/391/CEE, 86/179/CEE and 86/199/CEE) to ensure the health of its users. Acceptable PTEs concentration targets depend on, product users characteristics, with being children more vulnerable to metals toxicity; the amount of product applied; and body part of application (e.g., legs vs. face); the presence of emollients and/or penetration enhancers; and the application duration on the skin (Health Canada, 2012).

Sediment samples PTEs content is presented in Table 5. Results obtained, when compared to other studies in Ria de Aveiro sediments (Cabral-Pinto et al., 2020), suggesting a possible PTEs accumulation. In general, chemical composition of minor elements of total sample and silt fraction analysis revealed a similarity range of concentration values within each element. Exception, in As concentration in both fractions ($p < 0.05$) being only detected in two samples of silt fraction. Emphasis in total sample A1c, with an outlier value possibly related to allochthonous coarser materials introduced into the artificial beach area. Sample A1b also presented a high Cr content, while Cu revealed the higher concentration in sample A1c, like Zr in sample A2a. Sediment texture and natural metal concentrations usually present significant correlations, where sediment grain size plays a significant role in PTEs mobility in

**Table 5** Chemical composition of minor elements (mg/kg) of total sample and silt fraction

| ID | As | Cd | Co | Cr | Cu | Ni | Pb | Zn | Zr |
|---|---|---|---|---|---|---|---|---|---|
| *Total sample* | | | | | | | | | |
| A1a | 20.9 | 16.2 | 11.7 | 69.6 | 16.0 | 14.6 | 59.8 | 18.0 | 60.0 |
| A1b | 15.6 | 35.3 | 12.0 | 210.0 | 15.5 | 13.9 | 51.8 | 14.5 | 80.2 |
| A1c | 86.6 | 4.6 | 6.9 | 16.0 | 14.6 | nd | 34.6 | nd | 15.2 |
| A1d | 11.7 | 8.2 | 11.0 | 40.3 | 13.0 | 11.5 | 68.8 | 5.8 | 72.8 |
| A2a | 49.9 | 5.3 | 9.2 | 81.9 | 15.0 | 9.9 | 64.3 | 25.3 | 31.8 |
| A2d | 36.2 | 12.8 | 12.1 | 88.4 | 25.2 | 13.5 | 70.6 | 18.9 | 51.0 |
| *Silt fraction* | | | | | | | | | |
| A1a | nd | 9.3 | 20.7 | 90.8 | 36.0 | 27.4 | 80.0 | nd | 27.9 |
| A1b | nd | 12.1 | 14.2 | 77.0 | 18.2 | 25.0 | 66.6 | 9.2 | 28.4 |
| A1c | nd | 10.5 | 12.9 | 72.5 | 84.6 | 28.2 | 70.4 | 49.8 | 39.4 |
| A1d | 25.5 | nd | 15.2 | 70.2 | 23.5 | 21.3 | 87.5 | 34.6 | 63.0 |
| A2a | 27.6 | 4.4 | 10.1 | 75.2 | 21.1 | 18.0 | 76.1 | 56.5 | 210.0 |
| A2d | nd | 32.3 | 11.6 | 74.9 | 21.2 | 20.4 | 76.2 | 10.0 | 97.8 |

*nd* not detected.

aquatic ecosystems (Gloaguen et al., 2021). According to Magno et al. (2012) contaminants have lower mobility in silty and/or clayey materials, promoting its accumulation, while in sandy materials its mobility is high.

Due to the difficulty of guidelines for peloids application, soils threshold (TEL) and probable (PEL) effect levels defined to assess pollutants ecotoxicology in sediments, was used (Long & MacDonald, 1998). Below TEL values adverse effects are not expected to occur. In this study, As concentration is above PEL guidelines in total sample and silt fractions, the latter with less significance (Table 6). Cd concentration in both fractions is above PEL guidelines. The remaining elements show no incidence of toxicity in the sediment samples.

Toxic risk index (TRI) has TEL and PEL in consideration (Table 7). Elements Cr, Cu, Ni, Pb and Zn not revealed toxic risk in both fractions. Nevertheless, As and Cr toxic risk index vary by sample and fraction. As presented low toxic risk in total sample A1c while the remaining total samples and the silt fraction ones didn't presented TRI higher than limit. Total samples Cd TRI did not revealed toxic risk in A1c and A2a, low TRI in A1d, and moderate toxic risk in A1a and A2d. Very high Cd toxic risk was uncovered in total sample A1b. Silt fraction sample A2d was considered with very high Cd toxic risk, while A1d and A2a presented no toxic risk, A1a and A1c low TRI and A1b moderate TRI. PTEs that mostly contributed to total TRI were As and Cd, especially in total sample, the one used for dermal applications. Total sample A1b and silt fraction A2d were the ones with higher TRI, followed by total samples A1a and A2d. Particularly, silt fractions A1d and A2a are the ones with lower TRI, what can be related to the low As and Cd TRI.

Particularly, the threshold of the total sample analysis, A1c and A1b was very high As and Cd CF. All other samples revealed low, moderate, or high contamination factor (Table 8). Silt fraction sample A2d

**Table 6** Incidence of toxicity (in %) on the sediment samples.

| var | <TEL | >TEL <PEL | >PEL |
|---|---|---|---|
| *Total sample* | | | |
| As | 0.0 | 15.4 | 30.8 |
| Cd | 0.0 | 0.0 | 46.2 |
| Cr | 7.7 | 30.8 | 7.7 |
| Cu | 46.2 | 0.0 | 0.0 |
| Ni | 46.2 | 0.0 | 0.0 |
| Pb | 7.7 | 38.5 | 0.0 |
| Zn | 46.2 | 0.0 | 0.0 |
| *Silt fraction* | | | |
| As | 30.8 | 0.0 | 15.4 |
| Cd | 7.7 | 0.0 | 38.5 |
| Cr | 0.0 | 38.5 | 7.7 |
| Cu | 30.8 | 15.4 | 0.0 |
| Ni | 0.0 | 46.2 | 0.0 |
| Pb | 0.0 | 46.2 | 0.0 |
| Zn | 46.2 | 0.0 | 0.0 |

**Table 7** Toxic Risk Index on the sediment samples.

| ID | $TRI_{As}$ | $TRI_{Cd}$ | $TRI_{Cr}$ | $TRI_{Cu}$ | $TRI_{Ni}$ | $TRI_{Pb}$ | $TRI_{Zn}$ | TRI |
|---|---|---|---|---|---|---|---|---|
| *Total* | | | | | | | | |
| A1a | 1.9 | 13.8 | 1.0 | 0.2 | 0.5 | 0.9 | 0.1 | 18.3 |
| A1b | 1.4 | 30.0 | 3.0 | 0.2 | 0.4 | 0.8 | 0.1 | 36.0 |
| A1c | 7.8 | 3.9 | 0.2 | 0.2 | 0.0 | 0.5 | 0.0 | 12.7 |
| A1d | 1.0 | 7.0 | 0.6 | 0.2 | 0.4 | 1.1 | 0.0 | 10.2 |
| A2a | 4.5 | 4.5 | 1.2 | 0.2 | 0.3 | 1.0 | 0.1 | 11.8 |
| A2d | 3.2 | 10.9 | 1.3 | 0.4 | 0.4 | 1.1 | 0.1 | 17.4 |
| *Silt* | | | | | | | | |
| A1a | 0.0 | 7.9 | 1.3 | 0.5 | 0.9 | 1.2 | 0.0 | 11.8 |
| A1b | 0.0 | 10.3 | 1.1 | 0.3 | 0.8 | 1.0 | 0.0 | 13.5 |
| A1c | 0.0 | 8.9 | 1.0 | 1.2 | 0.9 | 1.1 | 0.2 | 13.4 |
| A1d | 2.3 | 0.1 | 1.0 | 0.3 | 0.7 | 1.3 | 0.2 | 5.9 |
| A2a | 2.5 | 3.7 | 1.1 | 0.3 | 0.6 | 1.2 | 0.2 | 9.6 |
| A2d | 0.0 | 27.5 | 1.1 | 0.3 | 0.6 | 1.2 | 0.0 | 30.7 |

**Table 8** Contamination factor (CF) and contamination degree (CD) using TEL and PEL guidelines

| ID | TEL guideline | | | | | | | | PEL guideline | | | | | | | |
|---|---|---|---|---|---|---|---|---|---|---|---|---|---|---|---|---|
| | $CF_{As}$ | $CF_{Cd}$ | $CF_{Cr}$ | $CF_{Cu}$ | $CF_{Ni}$ | $CF_{Pb}$ | $CF_{Zn}$ | CD | $CF_{As}$ | $CF_{Cd}$ | $CF_{Cr}$ | $CF_{Cu}$ | $CF_{Ni}$ | $CF_{Pb}$ | $CF_{Zn}$ | CD |
| *Total sample* | | | | | | | | | | | | | | | | |
| A1a | 3.5 | 27.2 | 1.9 | 0.4 | 0.8 | 1.7 | 0.1 | 5.1 | 1.2 | 4.6 | 0.8 | 0.1 | 0.4 | 0.7 | 0.1 | 1.1 |
| A1b | 2.6 | 59.2 | 5.6 | 0.4 | 0.8 | 1.5 | 0.1 | 10.0 | 0.9 | 10.0 | 2.3 | 0.1 | 0.4 | 0.6 | 0.0 | 2.0 |
| A1c | 14.7 | 7.7 | 0.4 | 0.4 | 0.0 | 1.0 | 0.0 | 3.5 | 5.1 | 1.3 | 0.2 | 0.1 | 0.0 | 0.4 | 0.0 | 1.0 |
| A1d | 2.0 | 13.8 | 1.1 | 0.4 | 0.6 | 2.0 | 0.0 | 2.8 | 0.7 | 2.3 | 0.4 | 0.1 | 0.3 | 0.8 | 0.0 | 0.7 |
| A2a | 8.5 | 8.9 | 2.2 | 0.4 | 0.6 | 1.8 | 0.2 | 3.2 | 2.9 | 1.5 | 0.9 | 0.1 | 0.3 | 0.7 | 0.1 | 0.9 |
| A2d | 6.1 | 21.5 | 2.4 | 0.7 | 0.8 | 2.0 | 0.2 | 4.8 | 2.1 | 3.6 | 1.0 | 0.1 | 0.4 | 0.8 | 0.1 | 1.2 |
| *Silt fraction* | | | | | | | | | | | | | | | | |
| A1a | 0.0 | 15.6 | 2.4 | 1.0 | 1.5 | 2.3 | 0.0 | 3.3 | 0.0 | 2.6 | 1.0 | 0.2 | 0.8 | 0.9 | 0.0 | 0.8 |
| A1b | 0.0 | 20.3 | 2.1 | 0.5 | 1.4 | 1.9 | 0.1 | 3.8 | 0.0 | 3.4 | 0.9 | 0.1 | 0.7 | 0.7 | 0.0 | 0.8 |
| A1c | 0.0 | 17.6 | 1.9 | 2.4 | 1.6 | 2.0 | 0.4 | 3.7 | 0.0 | 3.0 | 0.8 | 0.4 | 0.8 | 0.8 | 0.2 | 0.8 |
| A1d | 4.3 | 0.2 | 1.9 | 0.7 | 1.2 | 2.5 | 0.3 | 1.6 | 1.5 | 0.0 | 0.8 | 0.1 | 0.6 | 1.0 | 0.1 | 0.6 |
| A2a | 4.7 | 7.4 | 2.0 | 0.6 | 1.0 | 2.2 | 0.5 | 2.6 | 1.6 | 1.2 | 0.8 | 0.1 | 0.5 | 0.8 | 0.2 | 0.8 |
| A2d | 0.0 | 54.2 | 2.0 | 0.6 | 1.1 | 2.2 | 0.1 | 8.6 | 0.0 | 9.2 | 0.8 | 0.1 | 0.6 | 0.8 | 0.0 | 1.6 |

displayed very high Cd CF, while remaining samples are mostly classified with low to moderate contamination. Probable effect suggested very high contamination factor for Cd in total sample A1b and in silt fraction A2d. TEL guideline, suggested that total sample A1b presented the largest contribution to the total CD, followed by silt fraction A2d, which was classified with moderate contamination.

Considering RAIS (2022) soils risk guidelines for dermal contact, the use of the studied samples in dermal applications do not pose a risk of dermal systemic toxicity (non-carcinogenic outcomes), with PTEs concentrations being considered negligible for both children (0.008 to 0.056) and adults (0.001 to 0.009). Dermal carcinogenic risk is absent considering Cr, Co, Cu, Ni, Pb, Zn and Zr concentrations in all samples. Nevertheless, there is a risk due to As concentration in samples A1c, A2a and A2d, with 3.38E−06, 1.95E−06 and 1.41E−06, respectively. The highest risk was posed by A1c sample, reflecting the influence of allochthonous materials introduced during the beneficiation works of the pond. Arsenic desorption from metal oxy-hydroxides in alkaline environments, evaporation and the presence of As-rich saline waters are important factors of As enrichment (Dehbandi et al., 2019). These processes may explain the higher As concentrations in Area 2 samples, collected in small closed ponds with introduction of alkaline salted waters submitted to evaporation.

## Conclusions

This study aimed the textural, mineral, and chemical characterization of sediments used for peloterapy in a Portuguese SPA with two main areas for its users. Area 1 textural, mineral, and chemical analysis revealed significant variations before and after improvement works that occurred on its artificial beach. It was recorded an increase of particles grain size and PTEs concentration after the introduction of allochthonous materials. Area 2 sediments, with now beneficiation works but with seasonal salt production, revealed thinner particle sizes. Samples collected in Area 1 presented higher quartz content, while samples collected in Area 2 had higher halite mineral content. Illite was the main mineral phase present in the clay fraction. Potential toxic elements study revealed that Cd, followed by As, were the elements with highest toxicity incidence, given their concentrations above the probable effect guideline values, being the major contributors to toxic risk index, contamination factor, and contamination degree. Additionally, As represented a carcinogenic dermal risk in three samples (> 1.00E−06).

To consider, or not, the applicability of these sediments in pelotherapy applications is required additional specific analyses capable of evaluating its potential therapeutic properties. For that, this research needs further studies to understand dermal bioaccessibility of potentially toxic elements and to determine properties that define its application (e.g., abrasiveness, consistency limits, plasticity index, cooling time), what is being undertaken. Also, the analysis of the waters of the sampling areas is important to understand their quality and suitability in peloids maturation.

**Author contributions** LA: sampling, formal analysis, writing—original draft; CC: sampling, conceptualization, funding, methodology, formal analysis, supervision, writing—original draft. FR: funding, formal analysis, supervision, writing—review and editing.

**Funding** Authors are grateful to FCT for the financial support to Research Unit GeoBioTec (UID/GEO/04035/2019+UIDB/04035/2020).

**Data availability** Data used is available on the manuscript.

**Declarations**

**Competing interests** The authors declare no known competing financial interests or personal relationships that could have appeared to influence the work reported in this paper.

**Ethical approval** This research study doesn't involve animals.

**Consent to participate** This research study doesn't involve humans.

**Consent to publish** This research study doesn't involve individual person's data in any form.

## References

Abrantes, I., Rocha, F., & Dias, J. A. (2005). Spatial distribution and composition of suspended sediments in Ria de Aveiro. *Thalassas an International Journal of Marine Sciences, 21*(1), 45–52.

Argenziano, G., Delfino, M., & Russo, N. (2004). Mud and baththerapy in the acne cure. *Clinical Trial, 155*(4), 121–125.

Avumadi, A., Gnandi, K., & Probst, J. L. (2019). Trace element distribution and enrichment in the stream sediments of the Lake Togo Watersheds (South of Togo). *Advances in Ecological and Environmental Research, 4*, 87–114.

Baschini, M. T., Pettinari, G. R., Vallés, J. M., Aguzzi, C., Cerezo, P., López-Galindo, A., Setti, M., & Viseras, C. (2010). Suitability of natural sulphur-rich muds from Copahue (Argentina) for use as semisolid health care products. *Applied Clay Science, 49*, 205–212. https://doi.org/10.1016/j.clay.2010.05.008

Bastos, C. M., Rocha, F., Cerqueira, Â., Terroso, D., Sequeira, C., & Tilley, P. (2020). Assessment of clayey peloid formulations prior to clinical use in equine rehabilitation. *International Journal of Environmental Research and Public Health, 17*(10), 3365. https://doi.org/10.3390/ijerph17103365

Brindley, G. W., & Brown, G. (1980) X-Ray Diffraction Procedures for Clay Mineral Identification. In G. W. Brindley, G. Brown (Eds.), *Crystal Structures of Clay Minerals and Their X-Ray Identification*. doi:https://doi.org/10.1180/mono-5

Burdige, D. J. (2007). Preservation of organic matter in marine sediments: Controls, mechanisms, and an imbalance in sediment organic carbon budgets? *Chemical Reviews, 107*, 467–485. https://doi.org/10.1021/cr050347q

Cabral-Pinto, M. M. S., Inácio, M., Neves, O., Almeida, A. A., Pinto, E., Oliveiros, B., & Ferreira da Silva, E. (2020). Human health risk assessment due to agricultural activities and crop consumption in the surroundings of an industrial area. *Exposure and Health, 12*, 629–640. https://doi.org/10.1007/s12403-019-00323-x

Carretero, M. I. (2020a). Clays in pelotherapy. A review. Part I: Mineralogy, chemistry, physical and physicochemical properties. *Applied Clay Science, 189*, 105526. https://doi.org/10.1016/j.clay.2020.105526

Carretero, M. I. (2020b). Clays in pelotherapy. A review. Part II: Organic compounds, microbiology and medical applications. *Applied Clay Science, 189*, 105531. https://doi.org/10.1016/j.clay.2020.105531

Codish, S., Abu-Shakra, M., Flusser, D., Friger, M., & Sukenik, S. (2005). Mud compress therapy for the hands of patients with rheumatoid arthritis. *Rheumatology International, 25*(1), 49–54. https://doi.org/10.1007/s00296-003-0402-4

Costa, C., & Rydin, C. J. (2001). Site investigation on heavy metals contaminated ground in Estarreja—Portugal. *Engineering Geology, 60*(1–4), 39–47. https://doi.org/10.1016/S0013-7952(00)00087-9

Dehbandi, R., Abbasnejad, A., Karimi, Z., Herath, I., & Bundschuh, J. (2019). Hydrogeochemical controls on arsenic mobility in an arid inland basin, Southeast of Iran: The role of alkaline conditions and salt water intrusion. *Environmental Pollution, 249*, 910–922. https://doi.org/10.1016/j.envpol.2019.03.082

Dias, J. M., Lopes, J. F., & Dekeyser, I. (1999). Hydrological characterisation of Ria de Aveiro lagoon, Portugal, in early summer. *Oceanologica Acta, 22*(5), 473–485. https://doi.org/10.1016/S0399-1784(00)87681-1

Dias, J. M., Lopes, J. F., & Dekeyser, I. (2000). Tidal propagation in Ria de Aveiro Lagoon, Portugal. *Physics and Chemistry of the Earth (b), 25*(4), 369–374. https://doi.org/10.1016/S1464-1909(00)00028-9

Dias, J. M., Lopes, J. F., & Dekeyser, I. (2003). A numerical system to study the transport properties in the Ria de Aveiro lagoon. *Ocean Dynamics, 53*, 220–231. https://doi.org/10.1007/s10236-003-0048-5

Fernández-Moreno, D., Sánchez-Castillo, P. M., Delgado, C., & Almeida, S. F. P. (2022). Diatom species that characterize Saline ponds (Southern Spain) with the description of

a New *Navicula* Species. *Wetlands, 42*, 14. https://doi.org/10.1007/s13157-021-01529-z

Gadelha, J. R., Rocha, C., Camacho, C., Eljarrat, E., Peris, A., Aminot, Y., Readman, J. W., Boti, V., Nannou, C., Kapsi, M., Albanis, T., Rocha, F., Machado, A., Bordalo, A., Valente, L. M. P., Nunes, M. L., Marques, A., & Almeida, C. M. R. (2019). Persistent and emerging pollutants assessment on aquaculture oysters (Crassostrea gigas) from NW Portuguese coast (Ria de Aveiro). *Science of Total Environment, 666*, 731–742. https://doi.org/10.1016/j.scitotenv.2019.02.280

Galhano, C., Rocha, F., & Gomes, C. (1999). Geostatistical analysis of the influence of textural, mineralogical and geochemical parameters on the geotechnical behaviour of the "Argilas de Aveiro" formation (Portugal). *Clay Minerals, 34*, 109–116. https://doi.org/10.1180/claymin.1999.034.1.12

Garzanti, E. (2019). Petrographic classification of sand and sandstone. *Earth-Science Reviews, 192*, 545–563. https://doi.org/10.1016/j.earscirev.2018.12.014

Glavaš, N., Mourelle, M. L., Gómez, C. P., Legido, J. L., Šmuc, N. R., Dolenec, M., & Kovač, N. (2017). The mineralogical, geochemical, and thermophysical characterisation of healing saline mud for use in pelotherapy. *Applied Clay Science, 135*, 119–128. https://doi.org/10.1016/j.clay.2016.09.013

Gloaguen, T. V., Motta, P. N. S. D., & Couto, C. F. (2021). A grain-size correlation for metal pollution indexes in river sediments. *International Journal of Sediment Research, 36*, 362–372. https://doi.org/10.1016/j.ijsrc.2020.10.005

Gomes, C. S. F. (2018). Healing and edible clays: A review of basic concepts, benefits and risks. *Environmental Geochemistry Health, 40*, 1739–1765. https://doi.org/10.1007/s10653-016-9903-4

Gomes, C. S. F., Carretero, M. I., Pozo, M., Maraver, F., Cantista, P., Armijo, F., Legido, J. L., Teixeira, F., Rautureau, M., & Delgado, R. (2013). Peloids and pelotherapy: Historical evolution, classification and glossary. *Applied Clay Science, 75–76*, 28–38. https://doi.org/10.1016/j.clay.2013.02.008

Håkanson, L. (1980). An ecological risk index for aquatic pollution control a sedimentological approach. *Water Research., 14*, 975–1001. https://doi.org/10.1016/0043-1354(80)90143-8

Health Canada. (2012). Guidance on Heavy Metal Impurities in Cosmetics. https://www.canada.ca/en/services/health.html (Accessed 18 May 2022).

Heiri, O., Lotter, A. F., & Lemcke, G. (2001). Loss on ignition as a method for estimating organic and carbonate content in sediments: Reproducibility and comparability of results. *Journal of Paleolimnology, 25*, 101–110. https://doi.org/10.1023/A:1008119611481

Hossain, M. B., Marshall, D. J., & Venkatramanan, S. (2014). Sediment granulometry and organic matter content in the intertidal zone of the Sungai Brunei estuarine system, northwest coast of Borneo. *Carpathian Journal of Earth and Environmental Sciences., 9*(2), 231–239.

Infarmed. (2008). Portuguese Pharmacopoeia. (9th ed) Infarmed, Lisbon.

Karakaya, M. Ç., Karakaya, N., & Bakir, S. (2011). Some properties and potential applications of the Na- and Ca-bentonites of ordu (N.E. Turkey). *Applied Clay Science, 54*, 159–165. https://doi.org/10.1016/j.clay.2011.08.003

Karakaya, M. Ç., Karakaya, N., Sarıoğlan, Ş, & Koral, M. (2010). Thermal muds of some spas in Turkey. *Applied Clay Science, 48*, 531–537. https://doi.org/10.1016/j.clay.2010.02.005

Kikouama, J. R. O., Konan, K. L., Katty, A., Bonnet, J. P., Baldé, L., & Yagoubi, N. (2009). Physicochemical characterization of edible clays and release of trace elements. *Applied Clay Science, 43*, 135–141. https://doi.org/10.1016/j.clay.2008.07.031

Long, E., Ingersoll, C., & Macdonald, D. (2006). Calculation and uses of mean sediment quality guideline quotients: A critical review. *Environmental Science & Technology, 40*(6), 1726–1736. https://doi.org/10.1021/es058012d

Long, E., & MacDonald, C. (1998). Recommended uses of empirically derived, sediment quality guidelines for marine and estuarine ecosystems. *Human and Ecological Risk Assessment, 4*(5), 1019–1039. https://doi.org/10.1080/10807039891284956

Lopes, J. F., Dias, J. M., Cardoso, A. C., & Silva, C. I. V. (2005). The water quality of the Ria de Aveiro lagoon, Portugal: From the observations to the implementation of a numerical model. *Marine Environmental Research, 60*, 594–628. https://doi.org/10.1016/j.marenvres.2005.05.001

Loska, K., Cebula, J., Pelczar, J., Wiechula, D., & Kwapuliński, J. (1997). Use of enrichment, and contamination factors together with geoaccumulation indexes to evaluate the content of Cd, Cu, and Ni in the Rybnik water reservoir in Poland. *Water, Air and Soil Pollution, 93*, 347–365.

Magno, M. C., Bergamin, L., Finoia, M. G., Pierfranceschi, G., Venti, F., & Romano, E. (2012). Correlation between textural characteristics of marine sediments and benthic foraminifera in higly anthropogenically-altered coastal areas. *Marine Geology, 315–318*, 143–161. https://doi.org/10.1016/j.margeo.2012.04.002

Martins, M. V. A., Frontalini, F., Laut, L. L. M., Silva, F. S., Moreno, J., Sousa, S., Zaaboub, N., El Bour, M., & Rocha, F. (2014). Foraminiferal biotipes and their distribution control in Ria de Aveiro (Portugal): A multiproxy approach. *Environmental Monitoring and Assessment, 186*, 8875–8897. https://doi.org/10.1007/s10661-014-4052-7

Martins, V., Ferreira da Silva, E., Sequeira, C., Rocha, F., & Duarte, A. C. (2010). Evaluation of the ecological effects of heavy metals on the asemblages of benthic foraminifera of the canals of Aveiro (Portugal). *Estuarine, Coastal and Shelf Science, 87*, 293–304. https://doi.org/10.1016/j.ecss.2010.01.011

Martins, V. A., Frontalini, F., Tramonte, K. M., Figueira, R. C. L., Miranda, P., Sequeira, C., Fernández-Fernández, S., Dias, J. A., Yamashita, C., Renó, R., Laut, L. L. M., Silva, F. S., Rodrigues, M. A., Bernardes, C., Nagai, R., Sousa, S. H. M., Mahiques, M., Rubio, B., Bernabeu, A., … Rocha, F. (2013). Assessment of the health quality of Ria de Aveiro (Portugal): Heavy metals and benthic foraminifera. *Marine Pollution Bulletin, 70*(1–2), 18–33. https://doi.org/10.1016/j.marpolbul.2013.02.003

Mascolo, N., Summa, V., & Tateo, F. (1999). Characterization of toxic elements in clays for human healing use. *Applied*

*Clay Science, 15*, 491–500. https://doi.org/10.1016/S0169-1317(99)00037-X

Mil-Homens, M., Vale, C., Raimundo, J., Pereira, P., Brito, P., & Caetano, M. (2014). Major factors influencing the elemental composition of surface estuarine sediments: The case of 15 estuaries in Portugal. *Marine Pollution Bulletin, 84*(1–2), 135–146. https://doi.org/10.1016/j.marpolbul.2014.05.026

Moreira, M. H., Queiroga, H., Machado, M. M., & Cunha, M. R. (1993). Environmental gradientes in a southern Europe estuarine system: Ria de Aveiro, Portugal implications for soft bottom macrofauna colonization. *Netherland Journal of Aquatic Ecology, 27*, 465–482. https://doi.org/10.1007/BF02334807

Munsell. (2009). Munsell soil color charts. Munsell Colour Company. Inc., Newburgh, USA.

Nissenbaum, A., Rullkötter, J., & Yechieli, Y. (2002). Are the curative properties of black mud from the dead sea due to the presence of bitumen (asphalt) or other types of organic matter? *Environmental Geochemistry and Health, 24*, 327–335.

Oliveira, A., Rocha, F., Rodrigues, A., Jouanneau, J., Dias, A., Weber, O., & Gomes, C. (2002). Clay minerals from the sedimentary cover from the Northwest Iberian shelf. *Progress in Oceanogaphy, 52*, 233–247. https://doi.org/10.1016/S0079-6611(02)00008-3

Özay, P., Karagülle, M., Kardeş, S., & Karagülle, M. Z. (2020). Chemical and mineralogical characteristics of peloids in Turkey. *Environmental Monitoring Assessment, 192*, 805. https://doi.org/10.1007/s10661-020-08777-2

Pastorinho, M. R., Telfer, T. C., Nogueira, A. J. A., Soares, A. M. V. M., & Ranville, J. F. (2012). An evaluation of trace metal distribution, enrichment factors and risk in sediments of a coastal lagoon (Ria de Aveiro, Portugal). *Environmental Earth Science, 67*, 2043–2052. https://doi.org/10.1007/s12665-012-1643-x

Potopova, M., & Charles, D. F. (2003). Distribution of benthic diatoms in U.S. rivers in relation to conductivity and ionic composition. *Freshwater Biology, 48*, 1311–1328. https://doi.org/10.1046/j.1365-2427.2003.01080.x

Pozo, M., Carretero, M. I., Pozo, E., Martin Rubi, J. A., & Maraver, F. (2010). Caracterización mineralógica y química de peloides españoles y argentinos: Evaluación de elementos traza potencialmente tóxicos. In: Maraver, F., Carretero, M.I. (Eds.), Libro de Resúmenes del II Congreso Iberoamericano de Peloides, Lanjarón, C.E.R.S-A., Madrid, pp. 37–38.

Quintela, A., Terroso, D., Da Silva, E., & Rocha, F. (2012). Certification and quality criteria of peloids used for therapeutic purposes. *Clay Mineralogy, 47*(4), 441–451. https://doi.org/10.1180/claymin.2012.047.4.04

RAIS (2022). The Risk Assessment Information System (RAIS). U.S. Department of Energy's Oak Ridge Operations Office (ORO): Oak Ridge, TN, USA. https://rais.ornl.gov/, last accessed 2022.

Rasul, A., & Al-Jaleel, H. (2022). Assessment of heavy metal pollution in clay fraction of the Euphrates river sediments, AlQaim, Haditha Area. *Western Desert Iraq. Iraqi Geological Journal, 55*(1A), 139–157. https://doi.org/10.46717/igj.55.1A.11Ms-2022-01-30

Ravaglioli, A., Fiori, C., & Fabbri, B. (1989). Biblioteca Tecnica Ceramica, In Faenza (Ed.) Materia Prime Ceramiche. Argille, materiali non argillosi e sottoprodotti industriali. (p.392).

Reeuwijk, L. P. V. (2002). *Procedures for Soil Analysis* (6th ed.). Technical Paper/International Soil Reference and Information Centre.

Resende, P., Azeiteiro, U., & Pereira, M. J. (2005). Diatom ecological preferences in a shallow temperature estuary (Ria de Aveiro, Western Portugal). *Hydrobiologia, 544*, 77–88. https://doi.org/10.1007/s10750-004-8335-9

Rocha, F., Silva, E., Bernardes, C., Vidinha, J., & Patinha, C. (2005). Chemical and mineralogical characterisation of the sediments from the Mira, Ilhavo and Ovar channels of Aveiro Lagoon (Portugal). *Ciencias Marinas, 31*(1B), 253–263. https://doi.org/10.7773/cm.v31i12.90

Santisteban, J. I., Mediavilla, R., López-Pamo, E., Dabrio, C. J., Zapata, M. B. R., García, M. J. G., Castano, S., & Martínez-Alfaro, P. E. (2004). Loss on ignition: A qualitative or quantitative method for organic matter and carbonate mineral content in sediments? *Journal of Paleolimnology, 32*(3), 287–299. https://doi.org/10.1023/B:JOPL.0000042999.30131.5b

Smith, S. L., MacDonald, D. D., Keenleyside, K. A., Ingersoll, C. G., & Field, J. (1996). A preliminary evaluation of sediment quality assessment values for freshwater ecosystems. *Journal of Great Lakes Research, 22*(3), 624–638. https://doi.org/10.1016/S0380-1330(96)70985-1

Teixeira, C., & Zbyszewski, G. (1976). Geological map of Portugal at scale 1:50000. Sheet 18-C–Aveiro. Serviços Geológicos de Portugal. Lisboa (in portuguese).

Tolomio, C., Ceschi-Berrini, C., Moschin, E., & Galzigna, L. (1999). Colonization by diatoms and anti-rheumatic activity of thermal mud. *Cell Biochemistry and Function, 17*, 29–33. https://doi.org/10.1002/(SICI)1099-0844(199903)17:1%3c29::AID-CBF808%3e3.0.CO;2-4

Tserenpil, S., Dolmaa, G., & Voronkov, M. G. (2010). Organic matters in healing muds from Mongolia. *Applied Clay Science, 49*, 55–63. https://doi.org/10.1016/j.clay.2010.04.002

Uddin, F. (2008). Clays, nanoclays, and montmorillonite minerals. *Metallurgical and Materials Transactions A, 39*, 2804–2814. https://doi.org/10.1007/s11661-008-9603-5

Veniale, F., Barberis, E., Carcangiu, G., Morandi, N., Setti, M., Tamanini, M., & Tessier, D. (2004). Formulation of muds for pelotherapy: Effects of 'maturation' by different mineral waters. *Applied Clay Science, 25*, 135–148. https://doi.org/10.1016/j.clay.2003.10.002

Vieira, C. M. F., Sanchez, R., & Monteiro, S. N. (2008). Characteristics of clays and properties of building ceramics in the state of Rio de Janeiro Brazil. *Construction and Building Materials, 22*(5), 781–787. https://doi.org/10.1016/j.conbuildmat.2007.01.006

Viseras, C., Gil, E. C., Borrego-Sánchez, A., Villén, F. G., Sánchez-Espejo, R., Cerezo, P., & Aguzzi, C. (2019). Clay minerals in skin drug delivery. *Clays and Clay Minerals, 67*(1), 59–71. https://doi.org/10.1007/s42860-018-0003-7

Vodyanitskii, Y. N., & Savichev, A. T. (2017). The influence of organic matter on soil color using the regression equations of optical parameters in the system CIE-L*a*b*.

*Annals of Agrarian Science, 15*, 380–385. https://doi.org/10.1016/j.aasci.2017.05.023

Williams, L. B., Haydel, S. E., Giese, R. F., & Eberl, D. D. (2008). Chemical and mineralogical characteristics of French green clays used for healing. *Clay and Clay Minerals, 56*(4), 437–452. https://doi.org/10.1346/CCMN.2008.0560405

Wu, G., Zhang, X., Zhang, C., & Xu, T. (2016). Mineralogical and morphological properties of individual dust particles in ice cores from the Tibetan Plateau. *Journal of Glaciology, 62*(231), 46–53. https://doi.org/10.1017/jog.2016.8

Zhang, G., Bai, J., Zhao, Q., Lu, Q., Jia, J., & Wen, X. (2016). Heavy metals in wetland soils along a wetland-forming chronosequence in the Yellow River Delta of China: Levels, sources and toxic risks. *Ecological Indicators, 69*, 331–339. https://doi.org/10.1016/j.ecolind.2016.04.042

Zhao, Q., Bai, J., Huang, L., Gu, B., Lu, Q., & Gao, Z. (2016). A review of methodologies and success indicators for coastal wetland restoration. *Ecological Indicators, 60*, 442–452. https://doi.org/10.1016/j.ecolind.2015.07.003